SWIFT OBSERVATIONS OF THE HIGHLY X-RAY VARIABLE NARROW-LINE SEYFERT 1 GALAXY RX J0148.3−2758

DIRK GRUPE,[1] KAREN M. LEIGHLY,[2] STEFANIE KOMOSSA,[3] PATRICIA SCHADY,[1,4]
PAUL T. O'BRIEN,[5] DAVID N. BURROWS,[1] AND JOHN A. NOUSEK[1]

ABSTRACT

We report on *Swift* observations of the narrow-line Seyfert 1 galaxy RX J0148.3−2758. It was observed for 41.6 ks in 2005 May and for 15.8 ks in 2005 December. On short as well as on long timescales, RX J0148.3−2758 is a highly variable source. It doubles its X-ray flux within 18–25 ks. The observation of 2005 December 9, which had a flux 4 times lower than during the 2005 May observations, shows a significant hardening of the X-ray hardness ratio compared with the 2005 May and December 20 and 21 observations. A detailed analysis of the X-ray spectra shows that we actually observe two spectral changes in RX J0148.3−2758: first, a decrease of the soft X-ray component between 2005 May and December 9, which is most likely due to an increase of the intrinsic absorber column, and second, a decrease of the hard X-ray flux in the December 20 and 21 observations. The soft X-ray spectral slope $\alpha_{X,\text{soft}} = 2.58^{+0.15}_{-0.12}$ during the high state in 2005 May agrees well with that measured by *ROSAT* ($\alpha_{X,\text{soft}} = 2.54 \pm 0.82$). This soft X-ray spectrum is superposed on a hard X-ray component with $\alpha_{X,\text{hard}} = 0.96^{+0.16}_{-0.14}$, which is consistent with the hard X-ray spectral slope $\alpha_{X,\text{hard}} = 1.11^{+0.16}_{-0.19}$ found by *ASCA*. The soft X-ray slope $\alpha_{X,\text{soft}} = 1.93^{+0.58}_{-0.42}$ measured during the December 9 observation agrees well with $\alpha_{X,\text{soft}} = 2.03^{+0.23}_{-0.20}$ measured from the *ASCA* observation when RX J0148.3−2758 was also in a low state. In contrast to the strong X-ray variability, the analysis of the *Swift* UV-Optical Telescope (UVOT) photometry from 2005 December of RX J0148.3−2758 shows no significant variability in any of the six UVOT filters. From the simultaneous X-ray and UV observations in 2005 December we measured the X-ray loudness α_{ox} and found it to vary between $\alpha_{\text{ox}} = 1.5$ and 1.8. Our *Swift* observations of RX J0148.3−2758 demonstrate the great potential that the multiwavelength observatory *Swift* has for active galactic nucleus science.

Key words: galaxies: active — galaxies: individual (RX J0148.3−2758) — galaxies: Seyfert

1. INTRODUCTION

Most of the power in the spectral energy distribution (SED) of an active galactic nucleus (AGN) is contained in the big blue bump (BBB; Shields 1978). As suggested by Walter & Fink (1993), the BBB may stretch from the UV into the soft X-ray regime. The soft X-ray part of the BBB may be UV photons from the accretion disk that are shifted into the soft X-ray band by Comptonization in the accretion disk corona (e.g., Pounds et al. 1995). Based on their sample of soft X-ray-selected *ROSAT* AGNs, Grupe et al. (1998a) showed that the BBB extends as far as the optical band and that sources with steeper X-ray spectra tend to have bluer optical spectra, suggesting that narrow-line Seyfert 1 galaxies (NLS1s) are the AGNs with the strongest BBB component. However, from a study of the *IUE* spectra of NLS1s, Rodríguez-Pascual et al. (1997) came to the conclusion that NLS1s have weaker UV emission than broad-line Seyfert 1 galaxies. All these studies, however, were hampered by the lack of simultaneous observations in the optical/UV and X-ray bands; the observations available frequently had been performed years

apart. This situation has changed with the availability of the multi-wavelength observatories *XMM-Newton* and *Swift*.

Swift (Gehrels et al. 2004) is a multiwavelength mission equipped with three telescopes that together cover the electromagnetic spectrum between 6000 Å and 150 keV: the Burst Alert Telescope (BAT; Barthelmy 2005), the X-Ray Telescope (XRT; Burrows et al. 2005), and the UV-Optical Telescope (UVOT; Roming et al. 2005). *Swift* was designed to chase gamma-ray bursts (GRBs) and was launched on 2004 November 20. At the low-energy side of *Swift*'s observing window, the UVOT covers the wavelength range between 1700 and 6000 Å. The UVOT is a sister instrument of *XMM-Newton*'s Optical Monitor (Mason et al. 2001), equipped with a similar set of filters (Mason et al. 2001; Roming et al. 2005). The XRT covers the 0.3–10.0 keV range and uses a CCD detector identical to the EPIC MOS on-board *XMM-Newton* (Turner et al. 2001). As described by Hill et al. (2004) the XRT operates in three observing modes: photon counting (PC), which is equivalent to the full-frame mode on *XMM-Newton*; window timing; and low-rate photodiode. Due to the nature of the *Swift* mission, the XRT switches automatically between the observing modes according to the brightness of a source. Only for specific purposes, e.g., in case of calibration observations, are the modes set manually in the observing schedule. The BAT is a coded-mask experiment that operates in the 15–150 keV energy range, at the high-energy part of *Swift*'s observing window. Although the main purpose of the *Swift* mission is to detect and observe GRBs, fill-in targets are used in the observing schedule to optimize the scientific return of the mission when GRBs are not observable. *Swift*'s UV and X-ray capabilities and rapid and flexible scheduling make it an ideal observatory to study AGNs.

[1] Department of Astronomy and Astrophysics, Pennsylvania State University, 525 Davey Lab, University Park, PA 16802; grupe@astro.psu.edu, dxb15@psu.edu, nousek@astro.psu.edu.

[2] Homer L. Dodge Department of Physics and Astronomy, University of Oklahoma, 440 West Brooks Street, Norman, OK 73019; leighly@nhn.ou.edu.

[3] Max-Planck-Institut für extraterrestrische Physik, Giessenbachstrasse, D-85748 Garching, Germany; skomossa@mpe.mpg.de.

[4] Mullard Space Science Laboratory, Holmbury St. Mary, Dorking, Surrey RH5 6NT, UK; ps@mssl.ucl.ac.uk.

[5] Department of Physics and Astronomy, University of Leicester, Leicester LE1 7R, UK; pto@star.le.ac.uk.

TABLE 1
Observation Log of RX J0148.3−2758

Observatory	Observation	T Start[a]	T Stop[a]	T_{exp}[b]	$\log L_X$[c]
Swift..	Segment 002[d]	2005 May 6 00:05	2005 May 6 24:00	7637	37.85[e]
	Segment 003[d]	2005 May 7 00:05	2005 May 9 22:58	21966	...
	Segment 004[d]	2005 May 11 00:27	2005 May 11 23:11	8840	...
	Segment 006[d]	2005 May 13 00:45	2005 May 13 10:26	3132	...
	Segment 008[d]	2005 Dec 7 00:34	2005 Dec 7 10:35	822	37.83
	Segment 009[d]	2005 Dec 9 12:17	2005 Dec 9 23:54	6346	37.27
	Segment 010[d]	2005 Dec 20 13:40	2005 Dec 20 23:32	5110	37.26
	Segment 011[d]	2005 Dec 21 01:01	2005 Dec 21 14:00	3506	37.21
ASCA	SIS 0, 1	1997 Jul 11 21:11	1997 Jul 13 03:07	33243	36.92
	GIS 2, 3	1997 Jul 11 21:11	1997 Jul 13 03:07	36381	...
ROSAT....................................	Pointed PSPC	1992 Jul 9 09:54	1992 Jul 10 01:16	6652	37.79
	RASS	1990 Jul 15 15:26	1990 Jul 16 07:28	89	37.87
	RASS	1990 Dec 28 01:11	1990 Dec 29 07:37	140	38.05
	RASS	1991 Jan 15 09:24	1991 Jan 17 07:49	274	38.00

[a] Start and end times are given in UT.
[b] Observing time given in seconds.
[c] Rest-frame 0.2–2.0 keV luminosity given in watts.
[d] The term "segment" is from the way Swift is scheduled. Swift is scheduled on a day-by-day basis. A segment contains the observations of a source of a single day (except during the weekends, when Swift is scheduled for 3 days).
[e] Average luminosity of segments 002–006.

With the launch of the X-ray satellite ROSAT (Trümper 1982) the X-ray energy range down to 0.1 keV became accessible for the first time. During the half-year ROSAT All-Sky Survey (RASS; Voges et al. 1999), a large number of sources with steep X-ray spectra were detected (Thomas et al. 1998; Beuermann et al. 1999; Schwope et al. 2000). About one-third to one-half of these sources are AGNs. Grupe (1996) and Grupe et al. (1998a, 2004c) found that about 50% of bright soft X-ray-selected AGNs are NLS1s (Osterbrock & Pogge 1985; Goodrich 1989). They turned out to be the class of AGN with the steepest X-ray spectra (e.g., Puchnarewicz et al. 1992; Boller et al. 1996; Grupe 1996; Grupe et al. 1998a, 2001, 2004c; Vaughan et al. 2001; Williams et al. 2002) and often show very strong X-ray variability (e.g., Boller et al. 1996; Nandra et al. 1997; Leighly 1999a; Turner et al. 1999; Grupe et al. 2001). NLS1s are AGNs with extreme properties that seem to be linked to one another: a steeper X-ray spectral index α_X correlates with the strength of the optical Fe II emission and anticorrelates with the widths of the broad-line region Balmer lines and the strength of the narrow-line region forbidden lines (e.g., Grupe 1996, 2004; Grupe et al. 1999; Laor et al. 1994, 1997; Sulentic et al. 2000). All these relationships are governed by a set of fundamental underlying parameters, usually called the Boroson & Green (1992) eigenvector 1 relation in AGNs. The most accepted explanation for these eigenvectors is the Eddington ratio L/L_{Edd} or the mass of the central black hole M_{BH} (Boroson 2002; Sulentic et al. 2000; Grupe 2004; Yuan & Wills 2003), in which NLS1s are AGNs with the highest Eddington ratios and smallest black hole masses for a given luminosity. The Eddington ratio has also been found to be correlated with the X-ray spectral slope α_X (Grupe 2004). Alternatively, this can also be interpreted as the age of an AGN in which NLS1s are AGNs in an early stage of their development (Grupe 1996, 2004; Mathur 2000).

RX J0148.3−2758 ($\alpha_{J2000.0} = 01^h48^m22^s.3$, $\delta_{J2000.0} = −27°58'26''$, $z = 0.121$) was discovered during the RASS as a bright and variable X-ray source (Grupe et al. 1998a; Thomas et al. 1998; Schwope et al. 2000). It was identified as a NLS1 by Grupe (1996) and Grupe et al. (1999). Besides a later 6.7 ks ROSAT PSPC observation (Grupe et al. 2001), RX J0148.3–2758 was also ob-

served for 34 ks by ASCA (Turner et al. 1999; Vaughan et al. 1999). The 2–10 keV ASCA light curve shows that the source is highly variable (Turner et al. 1999). Its 2–10 keV spectral slope $\alpha_{2–10\,keV} = 0.99 \pm 0.17$ is typical for a Seyfert 1 galaxy (Vaughan et al. 1999). In this paper we present our observations of RX J0148.3−2758 with Swift, and we compare those with the data previously taken by ROSAT and ASCA. RX J0148.3−2758 was one of the most X-ray variable AGNs in the soft X-ray-selected AGN sample of Grupe et al. (2001).

The outline of this paper is as follows: In § 2 we describe the Swift, ROSAT, and ASCA observations and the data reduction; in § 3 we present the results of the Swift data analysis; and in § 4 we discuss the results. Throughout the paper, spectral indices are quoted as energy spectral indices with $F_\nu \propto \nu^{-\alpha}$. Luminosities are calculated assuming a ΛCDM cosmology with $\Omega_M = 0.27$, $\Omega_\Lambda = 0.73$, and a Hubble constant of $H_0 = 75$ km s^{-1} Mpc^{-1} using the luminosity distances given by Hogg (1999). All errors are 1 σ unless stated otherwise.

2. OBSERVATIONS AND DATA REDUCTION

RX J0148.3−2758 was observed by Swift between 2005 May 5 and 13 (segments 002–006) for a total of 41.6 ks and between 2005 December 7 and 21 for 15.8 ks (segments 008–011). Table 1 lists the segment numbers of the Swift observations, the start and end times, the total observing times, and the 0.2–2.0 keV rest-frame luminosities. All XRT observations were performed in PC mode. The event files were created with the standard Swift XRT analysis task xrtpipeline version 0.9.9. For both spectral and temporal analysis, source counts between 0.3 and 10 keV were extracted from a circle with a radius of 50'', and background photons were extracted from a 100'' circle in a source-free region near the source. We created source and background spectra and event files using XSELECT version 2.3. Background-subtracted light curves were created by using ESO's Munich Image Data Analysis System (MIDAS) version 04Sep, as described in Nousek et al. (2006). The data were binned to have 250 source plus background photons per bin, except for the 2005 December 7 observation, for which we used a binning of 150 photons per bin. Note that on 2005 May 27 the Swift XRT
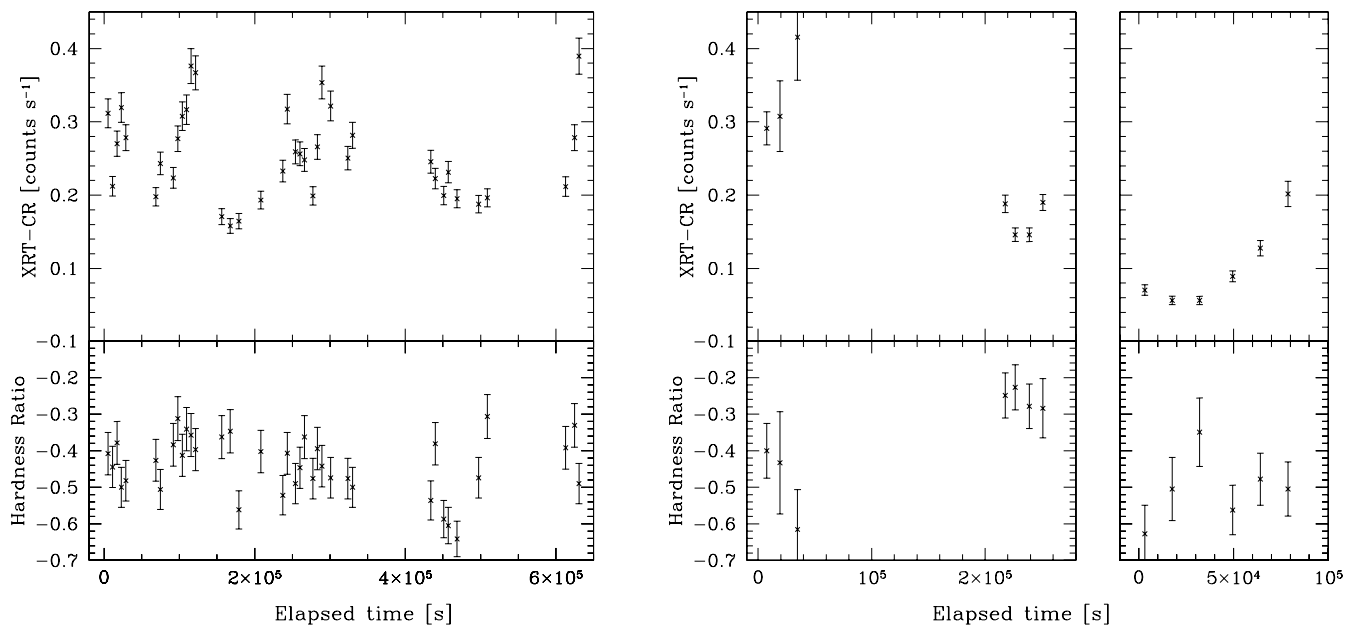
Fig. 1.—*Swift* XRT 0.3–10.0 keV light curves. *Left*, 2005 May observation; *middle*, December 7 and 9 observations; *right*, December 20 and 21 observations. Start times are 2005 May 6 00:05 UT, December 7 00:34 UT, and December 20 13:40 UT for the left, middle, and right panels, respectively. The start and end times of each segment are given in Table 1. The top panels display the count rate light curve, and the bottom panels display the light curve of the hardness ratio = $(H-S)/(H+S)$, where S and H are the number of photons in the 0.3–1.0 and 1.0–10.0 keV band, respectively.

detector was hit by a micrometeorite that caused some damage. In particular, the CCD columns DETX = 294 and 320 had to be turned off afterward. While our 2005 May and December 20 and 21 observations are not affected by those dead columns, the 2005 December 7 and 9 observations were in part. For the latter data sets, a correction was applied if the source felt on one of the dead columns to account for the loss of photons this caused. The spectra were rebinned using *grppha* version 3.0.0 to have at least 20 photons per bin and analyzed using XSPEC version 12.2.1 (Arnaud 1996). The auxiliary response files were created using the *Swift* analysis task *xrtmkarf*. We used the standard response matrix version 007 with grade selection 0–12. Due to the low count rate, the data were not affected by pileup.

Swift UVOT data were obtained during 2005 May 11 and 13 (segments 004 and 006) and 2005 December. The UVOT was blocked during the 2005 May 5 and 7 (segments 002 and 004) observations. The UV grism was used for the observations of 2005 May 11 and 13, and during 2005 December UVOT photometry was performed. Due to the ongoing calibration of the UV grisms and the requirement for well-calibrated UV grism data in our analysis, we do not present these data at this point, and we discuss only the UVOT photometry results of the 2005 December observations.

Observations were taken in the three optical and three UV filters available on the UVOT (Roming et al. 2005), with the exception of the 2005 December 7 (segment 008) observation, in which no *B*-band observations were made. This covers the wavelength range from 1700 to 6000 Å. There was a bright star ($B \sim$ 12.0 mag) about 10″ from RX J0148.3−2758 that made it necessary to carry out the UVOT photometry using a 4″.5 source extraction region. This is smaller than the 6″ and 12″ radii that are used for the optical and UV filters, respectively, for compatibility with the current effective area calibrations. An aperture correction was therefore applied to account for source photon counts that lay outside of this extraction region, in the wings of the point-spread function (PSF). The background region was taken from

an annulus around the source, off-centered by $\sim 7''$ to avoid excessive contamination from the nearby star. Source photon counts, magnitudes, and fluxes were then extracted using the UVOT tool *uvotmaghist* version 1.0 for every individual exposure taken in each filter, as well as from the co-added exposures within each segment number. All UVOT magnitudes were corrected for Galactic reddening with $E_{B-V} = 0.017$.

In order to be able to carry out broadband spectral fitting, source and background data files compatible with XSPEC were created from the co-added exposures from the 2005 December 9 (segment 009) observations. This was done using the tool *uvot2pha* version 1.1. This provided a single spectral file per filter. The same source and background extraction regions were used as before, and the exposure times in the headers were changed to normalize the count rates to the rates with the aperture correction taken into account.

The field of RX J0148.3−2758 was also observed by the BAT. However, a preliminary analysis of the BAT pointed and survey data does not show a detection of the source. So far more than 100 AGNs have been detected by the BAT, of which about 50 have had the results published (Markwardt et al. 2005).

RX J0148.3−2758 was observed by *ROSAT* with the PSPC (Pfeffermann et al. 1987) three times during the RASS for a total of 504 s and for 6.7 ks in a pointed observation (Table 1). Source counts were selected in a circular region with $R = 200''$. For the RASS observations background photons were taken from two circular regions with $R = 400''$ in the *ROSAT* scan direction (for details see Belloni et al. 1994). For the pointed observation the background was estimated from a close-by circular region with $R = 400''$. Spectra were rebinned to have at least a signal-to-noise ratio of 5 in each bin. The light curves were binned in 400 s bins. The *ROSAT* data were processed using EXSAS version Apr01 (Zimmermann et al. 1998).

ASCA observed RX J0148.3−2758 on 1997 November 7 for a total of 33.2 ks with its Solid-State Imaging Spectrometers (SISs) and 36.4 ks with the Gas Imaging Spectrometers (GISs)
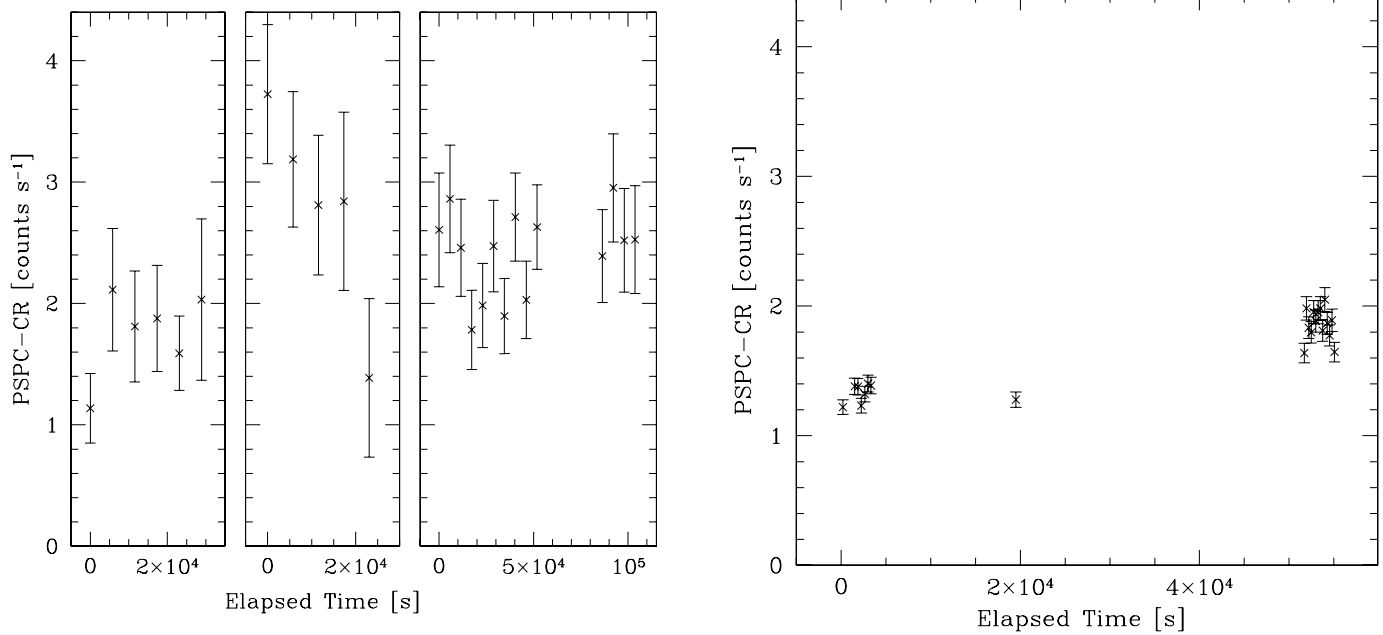
Fig. 2.—RASS and pointed observation light curves. The start times are 1990 July 15 15:26 UT, 1990 December 28 01:01 UT, and 1991 January 15 09:24 UT for the RASS observations (*left panels*) and 1992 July 9 09:54 for the pointed *ROSAT* PSPC observation (*right panel*).

on 1997 July 11 (Table 1). A standard configuration was used during the observation. The GISs were operated in PH mode throughout the observation. The SISs were operated in 1-CCD faint mode. The SIS energy gain was reprocessed using the latest calibration file (`sisph2pi_290301.fits`). We used standard criteria for reducing the *ASCA* data. For the SIS detectors, source photons were extracted from a circular region 3′.5 in radius, and for the GIS detectors, the source extraction region is 5′.25 in radius. In both cases the background was drawn from source-free regions of the detectors.

For spectral fitting, the spectra were grouped so that there were at least 20 photons per bin. It has been demonstrated that the SIS spectra suffered degradation during the mission. The SIS efficiency loss can be parameterized by adding additional absorption to the model, where the amount of additional absorption depends on the time of the observation.[6] For the time of RX J0148.3−2758, the appropriate additional column is 4.01×10^{20} cm^{-2}. We fit the SIS0 spectrum between 0.5 and 8.0 keV, the SIS1 spectrum between 1 and 0.8 keV, and the two GIS spectra between 0.8 and 8.0 keV.

3. RESULTS

3.1. *X-Rays*

3.1.1. *Light Curves*

Figure 1 (*left panel*) shows the *Swift* XRT light curve of RX J0148.3−2758 during the 2005 May observations (segments 002–006). The middle and right panels of the figure show the observations from 2005 December 7 and 9 (segments 008 and 009) and December 20 and 21 (segments 010 and 011), respectively. The XRT count rate light curves shown in Figure 1 (*top panels*) suggest that RX J0148.3−2758 is a highly variable source. In general, the AGN varies between ≈0.1 and 0.4 count s^{-1}. The most dramatic variability can be seen in the 2005 May light curve (Fig. 1, *left panel*), where the count rate doubled in 25 ks

between 90 and 115 ks, followed by a rapid drop between 120 and 150 ks by a factor of more than 2. A similar increase in count rate was also observed at the end of the 2005 May observation when RX J0148.3−2758 doubled its count rate within 18 ks. The 2005 December observations show that during the December 9 observation (*middle panel*) RX J0148.3−2758 became significantly fainter, with a count rate of about 0.18 counts s^{-1}. The AGN count rate fell by a further factor of 3 when it was reobserved on 2005 December 20 (segment 010, *right panel*). We do not know what happened between 2005 December 9 and 20, whether RX J0148.3−2758 remained in this low state during the 10 day gap, or whether further variability took place. By the end of segment 011 the count rate went back to its "normal" level, having increased by a factor of about 4 within 30 ks. The observations of 2005 December 21 were discontinued at the end of segment 011 due to the trigger of GRB 051221A (Parsons et al. 2005; Burrows et al. 2006), which superseded the RX J0148.3−2758 observation.
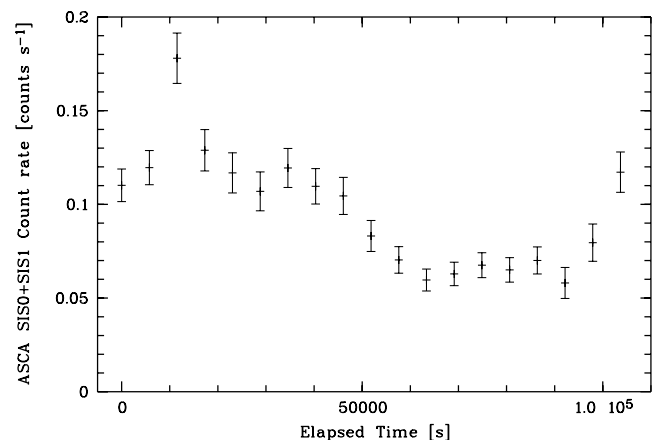

Fig. 3.—*ASCA* SIS0+SIS1 0.5–10 keV light curve. The start time was 1997 July 1 21:05 UT.
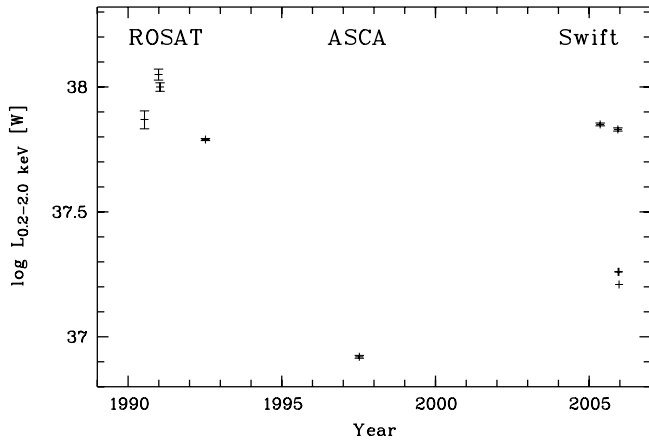
SWIFT OBSERVATIONS OF RX J0148.3−2758

FIG. 4.—Long-term light curve of RX J0148.3−2758. The luminosities are rest-frame 0.2–2.0 keV and are determined from unabsorbed fluxes based on the best-fit models as given in Tables 2 and 3.

The hardness ratio[7] plots suggest the presence of some spectral variability. While the hardness ratios during the December 7 and 20 and 21 observations are similar to those measured during May, the hardness ratio of the December 9 observations is significantly harder, suggesting a change in the X-ray spectrum.

The left panel of Figure 2 shows the RASS light curves, and the right panel displays the pointed *ROSAT* PSPC light curve. In both light curves RX J0148.3−2758 displays a similar variability, in agreement with the *Swift* XRT light curve (Fig. 1). RX J0148.3−2758 was one of the most variable of the soft X-ray-selected AGN sample of Grupe et al. (2001).

RX J0148.3−2758 was also observed by *ASCA* for a period of about 1 day. Light curves were extracted in the 0.5–10 keV band for the SIS detectors and the 0.8–10 keV band for the GIS detectors. The average net source count rates were 0.054, 0.043, 0.022, and 0.028 counts s^{-1} in the SIS0, SIS1, GIS2, and GIS3 detectors, respectively. The background fractions in the source

regions are estimated to be 20%, 22%, 36%, and 30% in the SIS0, SIS1, GIS2, and GIS3 detectors, respectively. The SIS0+ SIS1 net count rate light curve was binned by orbit and is displayed in Figure 3. The light curve shows that RX J0148.3− 2758 is varied by a factor of about 2, consistent with previous findings (e.g., Nandra et al. 1997), which found RX J0148.3− 2758 to show the largest excess variance among the AGNs observed by *ASCA* (Turner et al. 1999).

The long-term light curve shown in Figure 4 displays the complete set of X-ray observations performed on RX J0148.3−2758. The rest-frame 0.2–2.0 keV luminosities were derived from the unabsorbed fluxes determined from the best-fit spectral models as described in § 3.1.2. All luminosities are listed in Table 1. The light curve shows that during the *ASCA* observation RX J0148.3−2758 was in a low state, about 13 times fainter than during the RASS observation in 1990 December. During the *Swift* observation in 2005 May and at the beginning of the 2005 December observations, RX J0148.3−2758 was at a similar brightness as in the first RASS and the 1992 pointed *ROSAT* observations. By the end of the 2005 December *Swift* observations, RX J0148.3−2758 had become significantly fainter, only a factor of about 2 brighter than during the *ASCA* low state.

3.1.2. *Spectral Analysis*

Figure 5 displays the spectra of the 2005 May (*left*) and the 2005 December (*right*) observations. All spectra were initially fitted using a single absorbed power law with the absorption column density at $z = 0$ fixed to the Galactic value (1.50×10^{20} cm^{-2}; Dickey & Lockman 1990). A simple absorbed power law did not produce acceptable fits (Table 2). With the exception of the 2005 December 9 observations, all spectra require multicomponent spectral models such as blackbody-plus-power-law or a broken-power-law model, with an additional absorption component above the Galactic column density. A broken-power-law model, as well as a blackbody-plus-power-law model, yield similar χ^2/ν, and we cannot distinguish between the models. Using a blackbody model over a hard power-law component yields a temperature $kT \approx 100$–120 eV, which is typical for a NLS1 and agrees with the value $kT = 120$ eV found by *ASCA*
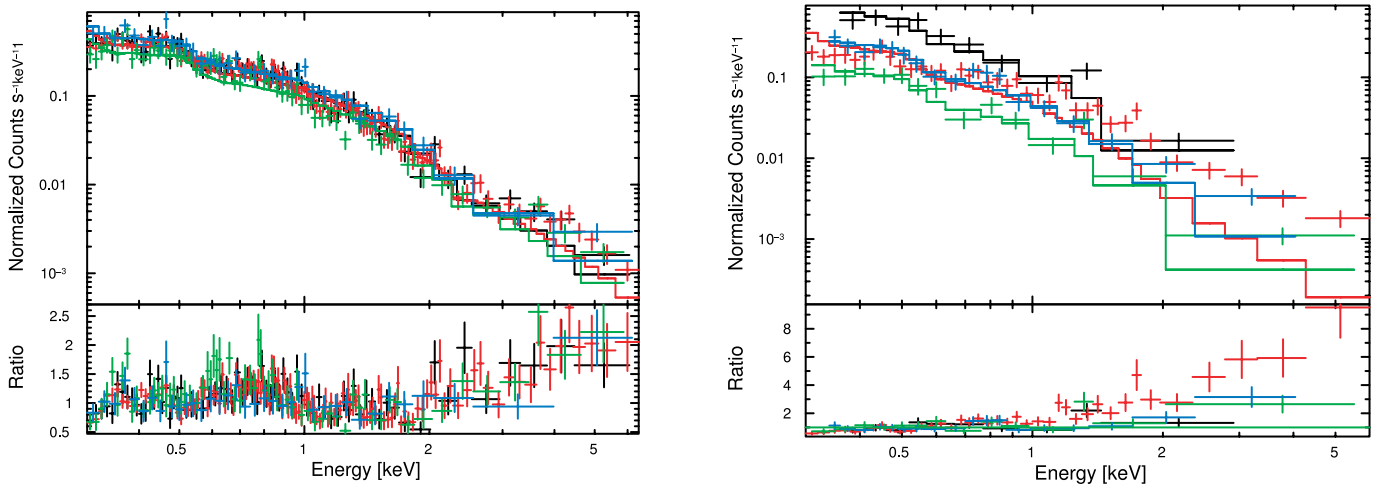
---

[7] The hardness ratio is defined by (hard−soft)/(hard+soft) with soft being the counts in the 0.3–1.0 keV band and hard being the counts in the 1.0–10.0 keV band.

FIG. 5.—*Swift* XRT spectra of RX J0148.3−2758. The 2005 May spectra (*left*) were fitted by a single power law with the absorption column fixed to the Galactic value. For the spectra of the 2005 December observations (*right*), the X-ray spectral slope was also fixed to $\alpha_X = 2.4$ (see text). The colors represent the spectra of different segments. *Left*: Segment 002, black; segment 003, red; segment 004, green; and segment 006, blue. *Right*: Segment 008, black; segment 009, red; segment 010, green; and segment 011, blue.

TABLE 2
Spectral Parameters of the Fits to the *Swift* XRT Spectra of RX J0148.3−2758

Observation Date	Model [a]	$N_{\rm H,Gal}$ (10^{20} cm^{-2})	$N_{\rm H,intr}$ (10^{20} cm^{-2})	$\alpha_{\rm X,soft}$ [b]	kT (eV)	$E_{\rm break}$ (keV)	$\alpha_{\rm X,hard}$	χ^2/ν
May 6	1	1.50 (fix)	...	1.84 ± 0.07	...	...	...	113/68
	1	$3.33^{+0.14}_{-0.12}$	...	$2.03^{+0.16}_{-0.15}$	...	...	...	107/67
	1	1.50 (fix)	$3.01^{+0.22}_{-0.19}$	$2.08^{+0.19}_{-0.17}$	...	...	...	106/67
	2	1.50 (fix)	...	...	126^{+8}_{-11}	...	$1.27^{+0.30}_{-0.21}$	83/65
	3	4.80 ± 1.16	...	2.28 ± 0.14	...	1.87 ± 0.25	0.95 ± 0.24	83/65
	4	1.50 (fix)	$7.95^{+0.25}_{-0.34}$	$2.59^{+0.21}_{-0.29}$	...	$1.80^{+0.16}_{-0.19}$	$0.85^{+0.35}_{-0.23}$	71/64
May 7	1	1.50 (fix)	...	1.82 ± 0.03	...	...	...	268/130
	1	2.77 ± 0.05	...	1.96 ± 0.05	...	...	...	258/129
	1	1.50 (fix)	$2.34^{+1.17}_{-1.09}$	$2.02^{+0.11}_{-0.10}$	...	...	...	254/129
	2	1.50 (fix)	...	...	118^{+5}_{-7}	...	$1.23^{+0.14}_{-0.13}$	179/127
	3	$4.85^{+0.93}_{-0.67}$	...	$2.30^{+0.12}_{-0.11}$	...	$1.72^{+0.15}_{-0.16}$	$1.01^{+0.18}_{-0.17}$	174/126
	4	1.50 (fix)	$7.61^{+0.20}_{-0.17}$	$2.61^{+0.19}_{-0.16}$	...	1.61 ± 0.14	$1.00^{+0.19}_{-0.13}$	146/126
May 11	1	1.50 (fix)	...	1.93 ± 0.05	...	...	...	155/67
	1	3.88 ± 0.09	...	2.13 ± 0.10	...	...	...	145/66
	2	1.50 (fix)	...	...	120 ± 7	...	$0.87^{+0.14}_{-0.23}$	84/65
	3	$6.18^{+1.81}_{-1.56}$	...	$2.53^{+0.25}_{-0.20}$	...	$1.75^{+0.25}_{-0.30}$	$0.69^{+0.42}_{-0.36}$	98/63
	4	1.50 (fix)	$7.88^{+0.36}_{-0.41}$	$2.75^{+0.32}_{-0.41}$	...	$1.70^{+0.33}_{-0.18}$	$0.68^{+0.33}_{-0.32}$	92/63
May 13	1	1.50 (fix)	...	1.83 ± 0.10	...	...	...	27/36
	1	$1.60^{+0.17}_{-0.15}$	...	$1.84x^{+0.20}_{-0.18}$	...	...	...	27/35
	2	1.50 (fix)	...	...	108^{+108}_{-102}	...	$1.64^{+0.25}_{-0.26}$	25/34
	3	1.50 (fix)	...	1.93 ± 0.08	...	1.70 (fix)	1.37 ± 0.23	23/34
	3	$3.01^{+1.80}_{-1.60}$	...	$2.10^{+0.21}_{-0.19}$	...	1.42 ± 0.50	1.47 ± 0.30	24/33
	4	1.50 (fix)	$3.42^{+0.33}_{-0.11}$	2.24 ± 0.16	...	$1.40^{+1.02}_{-3.24}$	$1.47^{+1.90}_{-3.11}$	23/32
May 6–13 [c]	1	1.50 (fix)	...	1.84 ± 0.03	...	...	...	567/304
	1	$2.92^{+0.55}_{-0.53}$	...	2.00 ± 0.07	...	...	...	546/303
	1	1.50 (fix)	$2.42^{+0.86}_{-0.82}$	2.05 ± 0.08	...	...	...	541/303
	2	1.50 (fix)	...	...	119 ± 4	...	$1.23^{+0.04}_{-0.06}$	386/299
	3	$4.96^{+0.68}_{-0.46}$	...	2.33 ± 0.08	...	1.76 ± 0.11	0.96 ± 0.13	386/300
	4	1.50 (fix)	$7.15^{+1.48}_{-1.21}$	$2.58^{+0.15}_{-0.12}$	...	$1.68^{+0.12}_{-0.14}$	$0.96^{+0.16}_{-0.14}$	347/301
Dec 7	1	1.50 (fix)	...	$2.17^{+0.27}_{-0.25}$	...	...	...	12/7
	2	1.50 (fix)	...	...	104 ± 16	...	$1.36^{+1.21}_{-1.36}$	10/6
	3	1.50 (fix)	...	2.26 ± 0.32	...	1.07 ± 1.39	1.86 ± 0.80	11/6
Dec 9	1	1.50 (fix)	...	$1.48^{+0.10}_{-0.09}$	...	...	...	30/37
	2	1.50 (fix)	...	...	100 ± 20	...	$1.29^{+0.22}_{-0.11}$	27/35
	3	1.50 (fix)	...	$1.60^{+0.38}_{-0.15}$	...	$1.28^{+4.30}_{-0.85}$	$1.26^{+0.29}_{-5.26}$	29/34
	3	$8.14^{+1.49}_{-1.36}$	...	2.33 (fix)	...	1.76 (fix)	0.96 (fix)	48/37
	4	1.50 (fix)	$2.92^{+6.07}_{-2.92}$	$1.93^{+0.58}_{-0.42}$	...	$1.16^{+0.30}_{-0.19}$	$1.27^{+0.27}_{-0.15}$	25/34
Dec 7 and 9 [c]	1	1.50 (fix)	...	1.57 ± 0.05	...	...	...	60/47
	2	1.50 (fix)	...	...	103^{+23}_{-19}	...	$1.23^{+0.23}_{-0.12}$	38/43
	3	$2.27^{+3.85}_{-1.80}$	...	$1.73^{+0.64}_{-0.23}$	...	$2.01^{+1.88}_{-0.65}$	$1.29^{+0.41}_{-0.71}$	54/43
	4	1.50 (fix)	$6.93^{+7.91}_{-5.96}$	$2.45^{+0.79}_{-0.73}$	...	$1.08^{+1.10}_{-0.15}$	$1.34^{+0.23}_{-0.61}$	41/42
Dec 20	1	1.50 (fix)	...	$2.07^{+0.21}_{-0.20}$	...	...	...	22/12
	4	1.50 (fix)	$2.86^{+6.80}_{-2.80}$	$2.47^{+0.62}_{-0.42}$	...	1.68 (fix)	0.96 (fix)	18/11
Dec 21	1	1.50 (fix)	...	$1.96^{+0.16}_{-0.15}$	...	...	...	29/17
	1	$4.44^{+3.25}_{-2.67}$	...	$2.33^{+0.43}_{-0.37}$	...	...	...	26/16
	2	1.50 (fix)	...	...	110 ± 14	...	$0.92^{+0.37}_{-0.56}$	16/15
	4	1.50 (fix)	$12.42^{+9.91}_{-6.72}$	$3.38^{+1.00}_{-0.73}$	...	$1.30^{+0.43}_{-0.26}$	$0.98^{+0.73}_{-0.95}$	12/14
Dec 20 and 21 [c]	1	1.50 (fix)	...	$2.00^{+0.13}_{-0.12}$	...	...	...	52/30
	1	$3.30^{+2.42}_{-2.10}$	...	$2.22^{+0.31}_{-0.21}$	...	...	...	57/29
	2	1.50 (fix)	...	...	101 ± 13	...	$1.13^{+0.37}_{-0.39}$	33/27
	3	$7.80^{+4.31}_{-3.60}$	...	$3.05^{+0.70}_{-0.55}$	...	$1.20^{+0.49}_{-0.20}$	$1.28^{+0.44}_{-0.73}$	32/27
	4	1.50 (fix)	$11.61^{+7.49}_{-5.73}$	$3.41^{+0.78}_{-0.64}$	...	$1.17^{+0.34}_{-0.17}$	$1.32^{+0.45}_{-0.52}$	30/27

[a] Model fit to the data: (1) Single power law with Galactic absorption, (2) blackbody plus power law with Galactic absorption, (3) broken power law with Galactic absorption, (4) broken power law with Galactic absorption and intrinsic absorption at $z = 0.121$.

[b] This spectral slope also refers to the 0.3–10.0 keV slope in case only a single power law has been used.

[c] Simultaneous fits in XSPEC.

(Table 3). A broken-power-law model simultaneously fitted to the 2005 May XRT spectra results in a soft X-ray spectral slope $\alpha_{\rm X,soft} = 2.58^{+0.15}_{-0.12}$, which is in good agreement with the results found by *ROSAT* (both the RASS and pointed observations; Table 3). The XRT hard X-ray spectral slope $\alpha_{\rm X,hard} = 0.96^{+0.16}_{-0.14}$ is also in good agreement with the hard X-ray spectral slope from

the *ASCA* data (Table 3). In addition to the phenomenological models, we fitted the partial covering absorber model *pcfabs*, the "warm" ionized absorber model *absori*, the reflection model *pexrav*, and the disk blackbody model to the 2005 May spectra. We found the *absori* and disk blackbody models to show no improvement over a simple power-law model, and the parameters

TABLE 3
Spectral Parameters of the Fits to the *ROSAT* and *ASCA* Spectra of RX J0148.3−2758

Mission	Observation	Model[a]	$N_{\rm H,Gal}$[b]	$N_{\rm H,intr}$[b]	$\alpha_{\rm X,soft}$[c]	kT[d]	$E_{\rm break}$[e]	$\alpha_{\rm X,hard}$	χ^2/ν
ASCA.................................	. . .	1	1.50 (fix)	. . .	$1.48^{+0.09}_{-0.08}$	. . .	. . .	. . .	254/237
	. . .	2	1.50 (fix)	. . .	. . .	127 ± 16	. . .	$1.10^{+0.13}_{-0.14}$	208/235
	. . .	3	1.50 (fix)	. . .	$2.03^{+0.23}_{-0.20}$	. . .	$1.36^{+0.16}_{-0.19}$	$1.11^{+0.16}_{-0.19}$	210/235
ROSAT..............................	RASS	1	1.50 (fix)	. . .	2.12 ± 0.11	. . .	. . .	. . .	30/23
	RASS	1	2.54 ± 0.82	. . .	2.62 ± 0.30	. . .	. . .	. . .	21/22
	Pointed	1	1.50 (fix)	. . .	1.88 ± 0.03	. . .	. . .	. . .	178/110
	Pointed	1	2.35 ± 0.22	. . .	2.25 ± 0.08	. . .	. . .	. . .	111/110

[a] Model fit to the data: (1) Single power law with Galactic absorption, (2) blackbody plus power law with Galactic absorption, (3) broken power law with Galactic absorption.
[b] Column density $N_{\rm H}$ given in units of 10^{20} cm^{-2}.
[c] This spectral slope also refers to the 0.3–10.0 keV slope in case only a single power law has been used.
[d] kT in units of eV.
[e] Broken-power-law break energy $E_{\rm break}$ in units of keV.

of the reflection model *pexrav* could not be constrained. However, the partial covering model *pcfabs* yielded reasonable results. We found the 2005 May spectra to be well fitted by a partial covering absorber with a column density $N_{\rm H} = 7.2^{+1.7}_{-1.3} \times 10^{22}$ cm^{-2}, a covering fraction $f = 0.80^{+0.03}_{-0.04}$, and a spectral index $\alpha_{\rm X} = 2.34 \pm 0.09$, where $\chi^2/\nu = 428/302$, which is significantly better than a single power-law fit as listed in Table 2.

Although the 2005 December 7 observations provided poorly constrained spectral fits due to the small number of photons (290 in 822 s), some interesting spectral variability is observed in the 2005 December data set. The hardness ratio light curve (Fig. 1, *bottom middle*) suggests that RX J0148.3−2758 had a similar spectrum as during the 2005 May and December 20 and 21 observations. However, a fit to the 6.3 ks observation from 2005 December 9 with a single absorber at $z = 0$ yields an absorption column density consistent with the Galactic value, suggesting there is no intrinsic absorption. Furthermore, an absorbed broken-power-law model yields a soft X-ray spectral slope $\alpha_{\rm X,soft} = 1.93^{+0.58}_{-0.42}$ flatter than during the 2005 May observations. To examine this spectral change, a Target-of-Opportunity observation was made with *Swift* on 2005 December 20 and 21. The spectral analysis of these data shows RX J0148.3−2758 to have once again become intrinsically absorbed, with $N_{\rm H,intr} = 11.6^{+7.5}_{-5.7} \times$

10^{20} cm^{-2}, and the soft X-ray spectral slope $\alpha_{\rm X,soft} = 3.41^{+0.78}_{-0.64}$ to have become significantly steeper. It is also interesting to note that between the 2005 May and December observations the best-fit spectral break from a broken-power-law model fit shifted toward softer energies. During the 2005 May observations the break energy was at $E_{\rm break} = 1.68^{+0.12}_{-0.14}$ keV, while during the 2005 December observations the break energy shifted to $E_{\rm break} \approx 1.2$ keV, in agreement with the break energy $E_{\rm break} = 1.36^{+0.16}_{-0.19}$ found by *ASCA* when RX J0148.3−2758 was also in a low state. As a result of the low number of photons in the December 9 observation, the parameters of a partial covering absorber were poorly constrained if all parameters were left to vary. However, by fixing the spectral index to the value during the 2005 May observations, $\alpha_{\rm X} = 2.33$, the fit resulted in a partial covering absorber with essentially the same covering fraction $f = 0.75^{+0.06}_{-0.09}$ as during the 2005 May observation but with a significantly lower $N_{\rm H} = 1.9^{+1.7}_{-0.9} \times 10^{22}$ cm^{-2} with $\chi^2/\nu = 35/35$. A partial covering absorber model fit to the December 20 and 21 spectrum found an increase of the absorption column of the partial covering absorber to $N_{\rm H} = 3.6^{+3.2}_{-1.4} \times 10^{22}$ cm^{-2}, a covering fraction $f = 0.87^{+0.06}_{-0.12}$, and $\alpha_{\rm X} = 3.98^{+0.48}_{-0.44}$, with $\chi^2/\nu = 30/27$.

Figure 6 (*left*) displays the spectra from the merged data sets of the 2005 May observations, the data set from December 9,
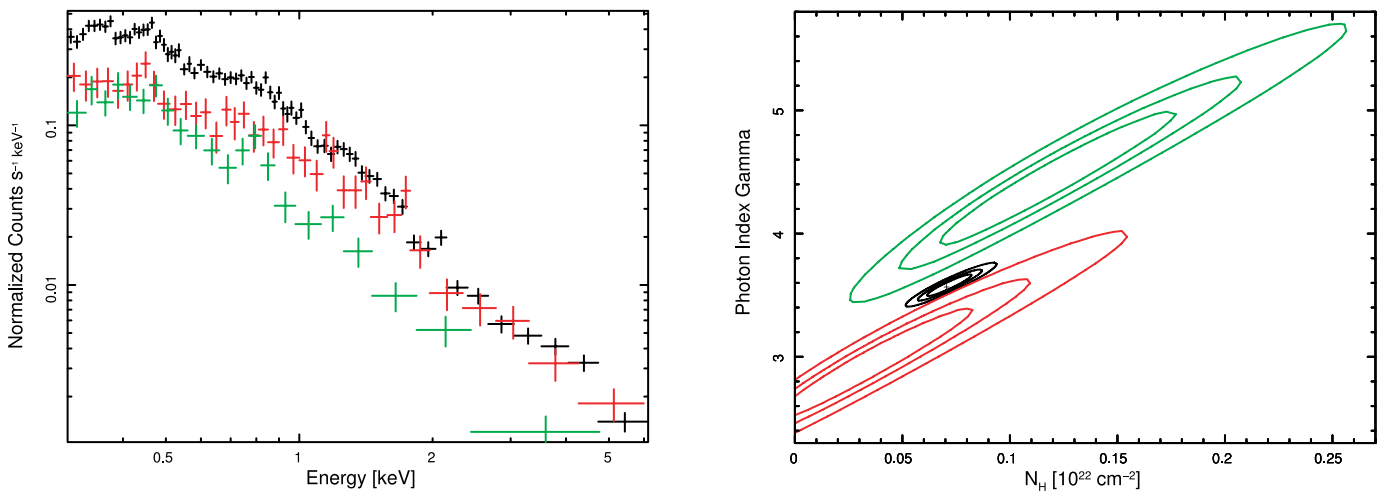

Fig. 6.—Comparison between the spectra of the 2005 May, December 9, and December 20 and 21 observations. The left panel displays the spectra with the average of the 2005 May spectra (segments 002–006; *black*), December 9 (segment 009; *red*), and December 20 and 21 (segments 010 and 011; *green*). The right panel shows the contour plot between the intrinsic column density $N_{\rm H,intr}$ and the soft X-ray photon index $\Gamma = \alpha_{\rm X,soft} + 1$ of the XRT spectra. The colors of the contours refer to the same segments as in the left panel.

TABLE 4
UVOT Photometry from the Co-added Images of RX J0148.3−2758

	Segment 008		Segment 009		Segment 010		Segment 011	
Filter	Mag.	Flux[a]	Mag.	Flux[a]	Mag.	Flux[a]	Mag.	Flux[a]
V..............	15.358 ± 0.062	26.90 ± 1.18	15.350 ± 0.018	27.10 ± 0.35	15.321 ± 0.020	27.84 ± 0.39	15.299 ± 0.017	28.41 ± 0.34
B..............	...	...	15.645 ± 0.015	33.45 ± 0.41	15.647 ± 0.017	33.37 ± 0.39	15.652 ± 0.088	33.24 ± 2.40
U..............	14.625 ± 0.042	47.19 ± 1.62	14.482 ± 0.011	53.80 ± 0.49	14.480 ± 0.013	53.91 ± 0.55	14.523 ± 0.030	51.81 ± 1.27
UVW1......	14.531 ± 0.031	64.62 ± 1.52	14.485 ± 0.009	67.39 ± 0.49	14.471 ± 0.011	68.29 ± 0.56	14.425 ± 0.024	71.25 ± 1.32
UVM2......	14.701 ± 0.031	74.77 ± 1.71	14.602 ± 0.010	81.85 ± 0.57	14.603 ± 0.011	81.78 ± 0.64	14.647 ± 0.024	78.57 ± 1.37
UVW2......	14.598 ± 0.018	112.15 ± 1.46	14.537 ± 0.007	118.60 ± 0.59	14.530 ± 0.008	119.39 ± 0.66	14.533 ± 0.006	119.11 ± 0.56

[a] The fluxes are given in units of 10^{-19} W m^{-2} Å^{-1}.

and the merged data set from December 20 and 21. The right panel shows the corresponding contour plots between the intrinsic column density and the photon index $\Gamma = \alpha_X + 1$. The lack of overlaps between the 2005 May, December 9, and December 20 and 21 observations suggests the presence of significant spectral variability in RX J0148.3−2758. The spectra in Figure 6 (*left*) show how the spectra change: compared with the 2005 May observations, the spectrum from December 9 has a similar hard X-ray flux but a significantly lower flux in the soft X-ray component. Then, in the December 20 and 21 observations, the soft X-ray component remained at a level similar to that of the December 9 observation. The hard X-ray flux, however, decreased by a factor of 4. By the end of the December 21 observation, RX J0148.3−2758 increased its 0.3–10.0 observed flux by a factor of 3 (Fig. 1).

The short-term variability we observed in RX J0148.3−2758 during the *Swift* observations seems to reflect the previous measurements by *ROSAT* and *ASCA*. During the high-state observations during the RASS and *ROSAT* pointed observations, the soft X-ray spectral slope was steep, with $\alpha_{X,\text{soft}} = 2.62$ and 2.25, respectively. For the spectral analysis of the *ASCA* data, we first constrain the power-law index by fitting the region between 2 and 5 keV with a power-law model. We obtain a good fit ($\chi^2 = 158$ for 173 degrees of freedom) and measure the energy index to be $1.16^{+0.27}_{-0.26}$. Next, we include the photons between 5 and 8 keV. The residuals show a slight excess that may indicate the presence of a reprocessing component. Indeed, when we plot the spectrum in this bandpass, we find that the photon index flattens to 2.01, although the difference is not significant. We add a narrow iron line at 6.4 keV but find no significant decrease in χ^2 ($\Delta\chi^2 = 1.78$). Allowing the line energy to vary yields a better fit, with $6.70^{+0.18}_{-0.24}$ keV, and a greater reduction in χ^2. However, the line equivalent width is very large (550 eV), and an *F*-test indicates that the change in χ^2 of 5.9 compared with the no-line model is not a significant improvement. Similarly, a broad line does not improve the fit significantly and produces a line with unphysically large equivalent width. We conclude that evidence for a line in these data is weak, most likely because of the low signal-to-noise ratio at high energies in the spectrum. Since there is some flattening that distorts the power law, we ignore the spectra above 5 keV henceforth. Note that due to the lower effective area in the *Swift* XRT at 6 keV, we were not able to identify the line with the XRT.

Next, we examine the spectrum at low energies. Extrapolating down to the lower limits described above, we find that the continuum subtly steepens toward low energies. Indeed, fitting between 1 and 5 keV gives an energy index of 1.25 ± 0.10, while fitting down to the lowest limits on the spectrum yields $1.48^{+0.09}_{-0.08}$. We conclude that there is a weak soft excess present. We can

model the soft excess with either a blackbody or a broken power law. The fit parameters between 0.5 and 5 keV are given in Table 3. The soft X-ray spectral slope $\alpha_{X,\text{soft}} = 2.03^{+0.23}_{-0.20}$ is in good agreement with $\alpha_{X,\text{soft}} = 1.93^{+0.58}_{-0.42}$ found during the 2005 December 9 observation by *Swift*.

3.2. UVOT Photometry

Table 4 summarizes the results of the analysis of the photometry of the co-added UVOT images. During segment 008, no observations of RX J0148.3−2758 were made in the *B* filter. Figure 7 displays the UVOT light curves of all six filters plus the XRT light curve from segments 008–011. The figure might suggest that there is some variability in the UV. However, a comparison with four field stars, as listed in Table 5, shows that the variations seen in the UVOT light curves are still within the error margins. Figure 8 displays the UVOT measurements of these comparison stars. This figure shows that the trends seen in the RX J0148.3−2758 UVOT light curves are also present in the light curves of the comparison stars. Therefore, we consider RX J0148.3−2758 not to be variable in the UV/optical band during the 2005 December observations. Figure 9 displays the UVOT *V* image of the field around RX J0148.3−2758 with the
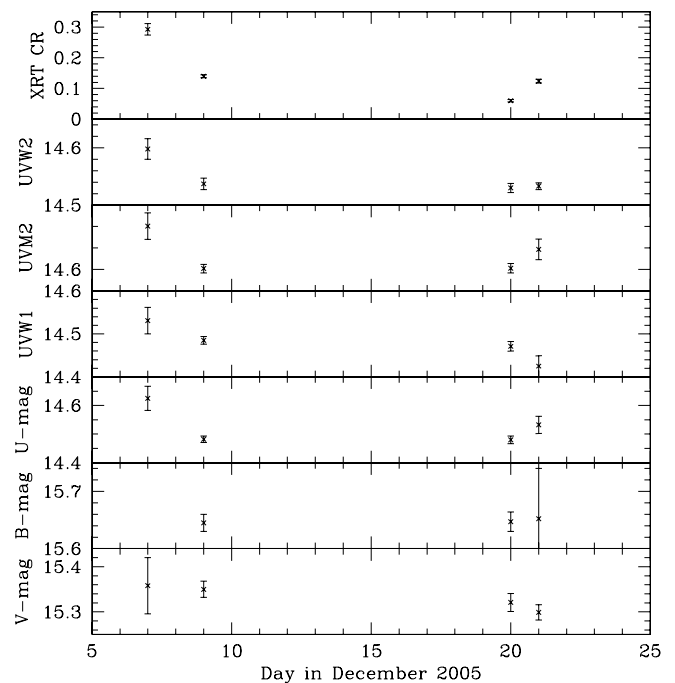

Fig. 7.—XRT and UVOT light curves.

TABLE 5
UVOT Photometry from the Co-added Images of the Four Comparison Stars

Star	Segment	V	B	U	UVW1	UVM2	UVW2
1.............................	008	13.102 ± 0.036	. . .	13.695 ± 0.038	15.063 ± 0.041	16.842 ± 0.087	16.804 ± 0.050
	009	13.072 ± 0.011	13.638 ± 0.018	13.600 ± 0.010	15.058 ± 0.012	16.667 ± 0.024	16.729 ± 0.017
	010	13.074 ± 0.012	13.634 ± 0.020	13.599 ± 0.012	15.046 ± 0.013	16.670 ± 0.027	16.728 ± 0.020
	011	13.074 ± 0.010	13.676 ± 0.010	13.600 ± 0.028	15.026 ± 0.031	16.672 ± 0.061	16.707 ± 0.016
2.............................	008	13.79 ± 0.037	. . .	14.29 ± 0.040	15.56 ± 0.056	16.96 ± 0.100	17.20 ± 0.063
	009	13.81 ± 0.011	14.38 ± 0.013	14.20 ± 0.011	15.60 ± 0.016	16.96 ± 0.029	17.20 ± 0.023
	010	14.02 ± 0.013	14.62 ± 0.014	14.42 ± 0.012	15.78 ± 0.019	17.17 ± 0.036	17.40 ± 0.028
	011	14.00 ± 0.011	. . .	. . .	. . .	. . .	17.36 ± 0.024
3.............................	008	15.09 ± 0.057	. . .	15.57 ± 0.061	16.70 ± 0.114	18.90 ± 0.382	18.41 ± 0.157
	009	15.09 ± 0.016	15.66 ± 0.015	15.50 ± 0.015	16.87 ± 0.032	18.14 ± 0.060	18.50 ± 0.053
	010	15.05 ± 0.018	15.63 ± 0.017	15.55 ± 0.017	16.84 ± 0.035	18.20 ± 0.069	18.50 ± 0.061
	011	15.08 ± 0.016	15.74 ± 0.092	15.54 ± 0.042	16.80 ± 0.080	18.27 ± 0.160	18.41 ± 0.048
4.............................	008	16.77 ± 0.162	. . .	16.89 ± 0.126	17.45 ± 0.196	18.34 ± 0.249	18.13 ± 0.120
	009	16.70 ± 0.038	17.02 ± 0.028	16.84 ± 0.023	17.52 ± 0.047	18.09 ± 0.056	18.38 ± 0.048
	010	16.69 ± 0.043	17.02 ± 0.031	16.85 ± 0.033	17.53 ± 0.053	18.12 ± 0.062	18.40 ± 0.053
	011	16.68 ± 0.036	17.16 ± 0.174	16.74 ± 0.073	17.45 ± 0.116	18.02 ± 0.131	18.33 ± 0.044

Note.—The light curves of these stars are shown in Fig. 8.

four comparison stars marked. In part, the variations seen in the UV light curves of RX J0148.3−2758 are due to the relatively small extraction radius of 4″.5 and the variable PSF of the UVOT. However, the lack of photometric data during the 2005 May observations provides us with no knowledge of the UV flux/magnitudes during a high state.

3.3. *Spectral Energy Distribution*

Figure 10 displays the SED of RX J0148.3−2758. The luminosities are the observed luminosities as given in Table 6. The *Swift* XRT data taken in 2005 May are shown as triangles, and the 2005 December 20 and 21 observations are represented by crosses. For the UVOT data, only the 2005 December data are shown. This AGN was not detected in the NRAO VLA Sky Survey (NVSS) or the FIRST radio catalogs. The far-infrared *IRAS* and near-infrared Two Micron All Sky Survey (2MASS) luminosities were derived with the GATOR catalog search engine at NASA/IPAC.[8] The *IRAS* luminosities deviate slightly from those given in Grupe et al. (1998a) due to the improved extraction software at IPAC.

We measured the optical–to–X-ray spectral slopes α_{ox}[9] of the 2005 December 9 and 20 and 21 observations from the SED plot (Fig. 10). During the December 9 observation we found a rest-frame $\alpha_{ox} = 1.53$. At a luminosity density $\log l_o = 22.78$ (W Hz^{-1}) and redshift $z = 0.121$, this value is in good agreement with the mean of the radio-quiet AGN *ROSAT* sample of Yuan et al. (1998a, 1998b) and Strateva et al. (2005) for the same redshift and luminosity intervals. Following the relation given in equation (4) in Strateva et al. (2005), we would expect $\alpha_{ox} = 1.42$. However, during the December 20 and 21 observation the source became more X-ray quiet with an $\alpha_{ox} = 1.81$. We have yet to analyze the grism data taken during 2005 May, when the source was in a high state. We therefore have no current measure of α_{ox} during this time period. Although the 2005 December UVOT observations show no significant variability, the value of α_{ox} during the observations of 2005 May cannot be determined

because we do not know what the flux in the UV filters was during this time period.

This NLS1 has been observed once before in the UV, in 1992 by *IUE* (SWP 45107). The spectrum is displayed in Figure 11 (*left*). Figure 11 (*right*) shows the optical spectrum of RX J0148.3−2758 taken in 1995 September at the ESO 1.52 m telescope in La Silla for a total of 4 hr. Details of this observing run are given in Grupe et al. (2004c). With FWHM(Hβ) = 1030 ± 100 km s^{-1} we derived a central black hole mass of $1.3 \times 10^7 \, M_\odot$ using equation (5) in Vestergaard & Peterson (2006). From the *IUE* spectrum shown in Figure 11 we derived FWHM(C IV) = 2300 km s^{-1}. By using the relation given in equation (7) in Vestergaard & Peterson (2006) we estimated the black hole mass $M_{BH} = 3.4 \times 10^7 \, M_\odot$. Both black hole mass estimates agree with each other within their uncertainties.

Estimated from these black hole masses, the Eddington luminosity is $(1.6–4.3) \times 10^{38}$ W. As described in Grupe et al. (2004c) we modeled the BBB by a power law with exponential cutoff plus an absorbed power law. This model is displayed in Figure 10. From the 2005 December 20 and 21 data we measured a bolometric luminosity $L_{bol} = 5 \times 10^{38}$ W, which is similar to the value given by Grupe et al. (2004c) based on the optical spectrum and the RASS data. This results in an Eddington ratio $L/L_{Edd} = 1–3$.

The [O III] lines can be separated into a narrow and a blue-shifted broad component. The broad [O III] lines are blueshifted by 600 ± 200 km s^{-1} with respect to the narrow [O III] and Hβ lines. Similar results on NLS1s have been previously reported by, e.g., Grupe & Leighly (2002), Zamanov et al. (2002), Aoki et al. (2005), and Bian et al. (2005).

4. DISCUSSION

In this paper we have presented the *Swift* observations of the highly variable NLS1 RX J0148.3−2758. In addition to the strong X-ray flux variability, our main results are composed of the spectral changes. We observed a hardening followed by a softening of the spectrum of RX J0148.3−2758 over a time during which the X-ray flux was on a continual decrease. Both types of spectral changes have been observed in AGNs, although the hardening of the X-ray spectrum with decreasing flux is more common (e.g., Gallo et al. 2004a; Dewangan et al. 2002; Lee

---

[8] See http://irsa.ipac.caltech.edu/applications/Gator/.
[9] The X-ray loudness is defined by Tananbaum et al. (1979) as $\alpha_{ox} = -0.384 \log (f_{2 \, keV}/f_{2500 \, Å})$.
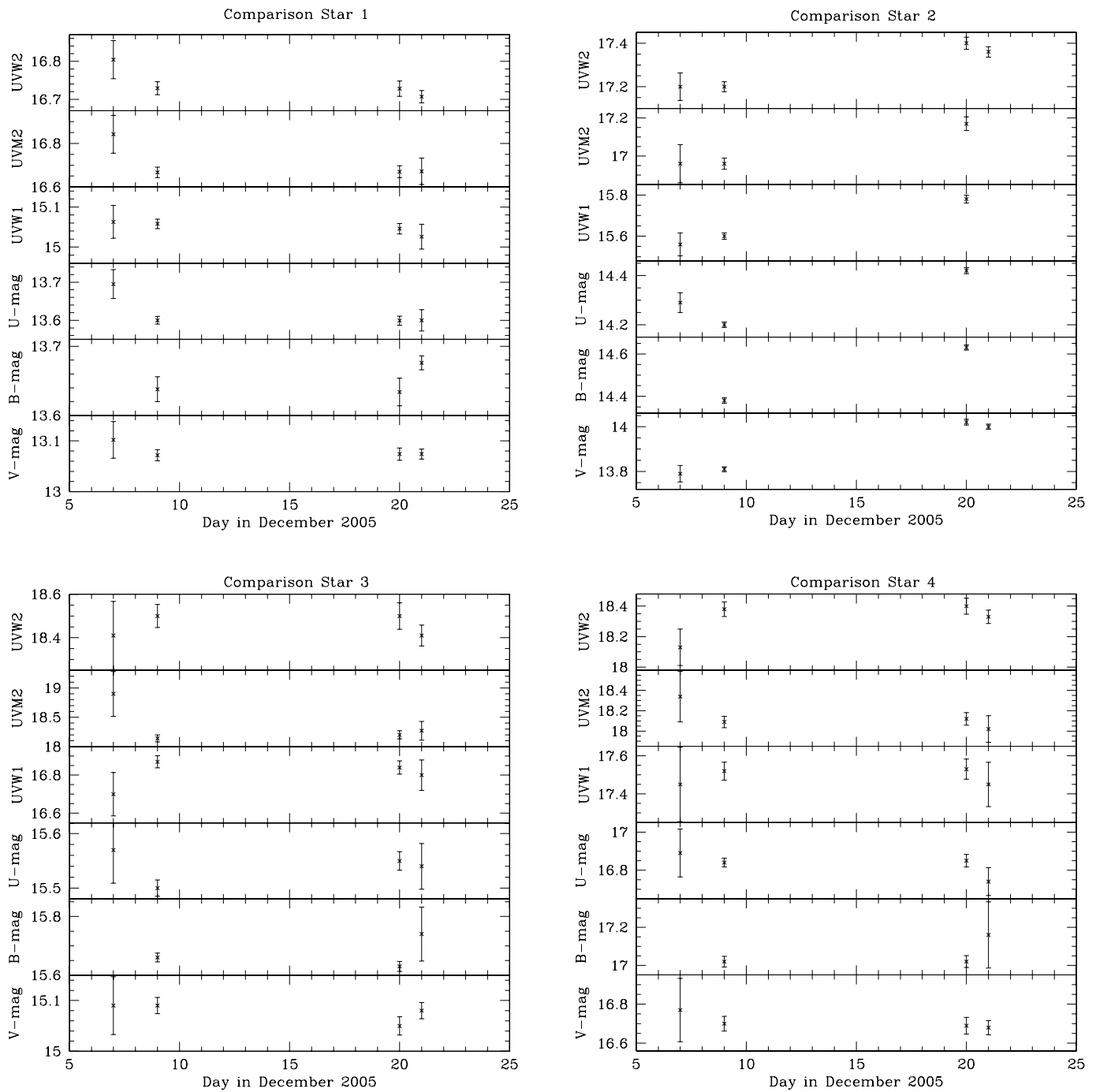
Fig. 8.—UVOT light curves of comparison stars 1–4 as given in Table 5 and displayed in Fig. 9.

et al. 2000; Chiang et al. 2000). However, softening of the X-ray spectrum with decreasing flux has been reported in, e.g., NLS1s RX J2217.9−5941 (Grupe et al. 2004a), RX J0134.2−4258 (Grupe et al. 2000; Komossa & Meerschweinchen 2000), PKS 0558−504 (Gliozzi et al. 2001), and 1H 0707−495 (Gallo et al. 2004b; Fabian et al. 2004).

A simple way to explain a hardening in the spectrum with decreasing observed X-ray flux is with a cold absorber cloud in the line of sight. Variable absorbers in AGNs are often observed in Seyfert galaxies, e.g., the Seyfert 2 sample of Risaliti et al. (2002), NGC 1365 (Risaliti et al. 2005), NGC 4388 (Elvis et al. 2004), the Seyfert 1.8 galaxy NGC 3786 (Komossa & Fink 1997b),

the Seyfert 1.5 galaxies NGC 4151 (Puccetti et al. 2004) and NGC 3227 (Komossa & Fink 1997a), or 1H 0419−577 (Pounds et al. 2004). A variable cold absorber could also, in part, provide a plausible explanation for the spectral variability between the 2005 May and December 9 observations. As listed in Table 2, we fitted an absorbed broken power law to the 2005 December 9 data, where all parameters were fixed to those determined from the 2005 May observations, except for the absorption column density and the normalization, which were allowed to vary. This provided a best-fit column density $N_H = (8.1 \pm 1.4) \times 10^{20}$ cm^{-2}, although there were strong residuals below 0.5 keV. Although NLS1s often resemble AGNs with only minor intrinsic absorption,

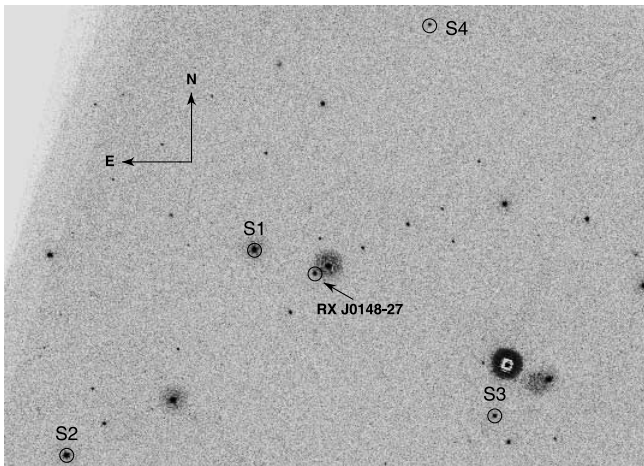Fig. 9.—UVOT *V* image of the field around RX J0148.3−2758. The four comparison stars listed in Table 5 are marked as S1–S4 in the figure.
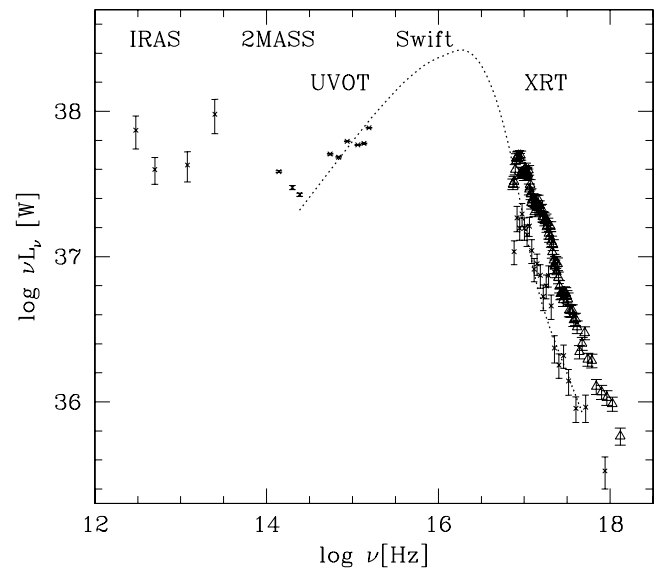

Fig. 10.—SED of RX J0148.3−2758. The luminosities are the observed luminosities as given in Table 6. The crosses represent the *Swift* UVOT and XRT data of the 2005 December 20 and 21 observations, and the triangles represent the XRT observations from 2005 May. The dotted line displays the power law plus exponential cutoff and absorbed-power-law model to describe the BBB.

this is not a true picture in general (e.g., Grupe et al. 1998b, 2004b). A different result is found if all parameters are left to vary. As listed in Table 2 and shown in Figure 6, N_H actually becomes consistent with the Galactic value, and the soft X-ray spectral index $\alpha_{X,soft}$ flattens out. However, in a fitting routine like XSPEC, N_H and the spectral index are not independent parameters. A larger value of the absorption column density N_H will result in a steeper spectral index, and vice versa. Given the column density observed on December 20 and 21, which was again on the order of 10^{21} cm^{-2}, we can conclude that the spectral change seen between the 2005 May and December 9 observations is most likely due to an increase in the absorber column density. A soft X-ray spectrum fitted by a spectral model can mimic a low column density, as shown by, e.g., Puchnarewicz et al. (1995) and Grupe et al. (1998a), even though the real column density is much larger.

A softening with decreasing X-ray flux can be caused by several processes, such as a change in the accretion disk corona (e.g., Grupe et al. 2000) or the presence of a variable ionized absorber (e.g., Komossa & Meerschweinchen 2000). Another possibility is the presence of a partial covering absorber, as discussed for, e.g., RX J2217.9−5941 (Grupe et al. 2004a), 1H 0707−495 (Gallo et al. 2004b; Tanaka et al. 2004), and Mrk 1239 (Grupe et al. 2004b). As an alternative, Fabian et al. (2004) discussed the variability observed in 1H 0707−495 in the context of X-ray reflection on an ionized disk. Of all these models only the partial covering absorber model yields reasonable results. Interestingly, the coverage fraction observed in the 2005 May, December 9, and December 20 and 21 observations remains the same, at around $f = 0.8$. The column density of the partial covering absorber follows the same trend as the cold absorber column density, suggesting that it is at a low value during the December 9 observation.

The soft X-ray slope $\alpha_{X,soft} = 2.58^{+0.15}_{-0.12}$ is rather steep even for a NLS1. The mean soft X-ray slope for the sample of 51 NLS1s from Grupe et al. (2004c) is $\alpha_X = 1.96$ with a standard deviation $\sigma = 0.41$ and $\alpha_X = 2.1$ for the sample taken from Boller et al. (1996). However, the hard X-ray spectral slope of $\alpha_X = 0.96^{+0.16}_{-0.14}$ is slightly flatter than that found in the sample of NLS1s from Leighly (1999b), who found a mean hard X-ray slope of $\alpha_X = 1.19 \pm 0.10$, and the sample from Brandt et al. (1997) with $\alpha_X = 1.15$. This is in better agreement with the values found for a broad-line Seyfert 1, for which Leighly (1999b) found $\alpha_X = 0.78 \pm 0.11$ and Brandt et al. (1997) found $\alpha_X = 0.87$. A possible explanation for this "discrepancy" is that

whereas the soft X-ray spectral slope is driven by the Eddington ratio L/L_{Edd}, the hard X-ray spectral slope is more dependent on the black hole mass. The Eddington ratio L/L_{Edd} is one of the highest in the sample from Grupe et al. (2004c), with $L/L_{Edd} = 4$. As shown by Grupe & Mathur (2004) and Mathur & Grupe (2005a, 2005b), NLS1s with a high Eddington ratio L/L_{Edd} deviate significantly from the M_{BH}-σ stellar velocity dispersion relation (e.g., Gebhardt et al. 2000; Ferrarese & Merritt 2000; Tremaine et al. 2002). With a FWHM([O III]) = 700 ± 500 and a black hole mass on the order of a few 10^7 $M_\odot$, RX J0148.3−2758 shows one of the most extreme deviations from the Tremaine et al. (2002) M_{BH}-σ relation.

RX J0148.3−2758 also shows a variation in its optical–to–X-ray spectral slope α_{ox}. While during the 2005 December 9 observations $\alpha_{ox} = 1.5$, during the December 20 and 21 observations RX J0148.3−2758 became X-ray weak with $\alpha_{ox} = 1.81$. Similar changes in α_{ox} have also been recently reported by Gallo (2006). Changes like these can explain in part the large scatter seen in the α_{ox} diagrams of, e.g., Yuan et al. (1998a, 1998b) and Strateva et al. (2005).

The *Swift* observations of RX J0148.3−2758 have shown the great potential of *Swift* for AGN science. The X-ray light curves are highly variable, in particular those of NLS1s, and require long-term coverage in a range of wavelengths. Due to its low-Earth orbit, *Swift* is very similar to *ROSAT* and *ASCA* but has the added advantage of being a multiwavelength observatory. Our study has shown the importance of simultaneous UV and X-ray observations over a time span of days, and *Swift* is the only observatory that can obtain such observations. Our observations of RX J0148.3−2758 use the multiwavelength capabilities of *Swift*, as well as its flexible observing scheduling. The simultaneous observations in the UVOT and XRT allow us to measure the X-ray loudness α_{ox} directly without assuming any optical/UV spectral slopes. We are also able to measure the total power in the big blue bump and therefore the bolometric luminosity directly. The strong change in its spectrum between the 2005 May and December 9 observations prompted us to execute further

TABLE 6
MEASUREMENTS OF THE SPECTRAL ENERGY DISTRIBUTION SHOWN IN FIG. 10

Observatory	Filter	λ_c[a]	$\log \nu$ (Hz)	Magnitude[b]	νL_ν[c]	Comments
NVSS	1.40 GHz	...	9.146	<1	...[d]	
IRAS	100 μm	100 μm	12.477	746 ± 190	7.41 ± 1.89	
	60 μm	60 μm	12.699	237 ± 50	3.98 ± 0.83	
	25 μm	25 μm	13.079	107 ± 25	4.27 ± 1.00	
	12 μm	12 μm	13.398	113 ± 30	9.55 ± 2.54	
2MASS.................................	K_s	2.159 μm	14.143	12.250 ± 0.026	3.85 ± 0.05	
	H	1.662 μm	14.302	13.399 ± 0.032	2.99 ± 0.10	
	J	1.235 μm	14.385	14.214 ± 0.025	2.67 ± 0.07	
UVOT	V	5460 Å	14.740	15.37 ± 0.02	5.08 ± 0.25	Segment 010
	B	4340 Å	14.840	15.66 ± 0.02	4.84 ± 0.24	Segment 010
	U	3450 Å	14.939	14.49 ± 0.01	6.22 ± 0.31	Segment 010
	UVW1	2600 Å	15.062	14.49 ± 0.01	5.88 ± 0.30	Segment 010
	UVM2	2200 Å	15.135	14.60 ± 0.01	6.01 ± 0.30	Segment 010
	UVW2	1930 Å	15.191	14.54 ± 0.01	7.70 ± 0.38	Segment 010

[a] Central wavelength of the filter.
[b] For the NVSS and the *IRAS* data we give the flux densities in units of mJy. All others are given in units of mag.
[c] Observed luminosities are given in units of 10^{37} W.
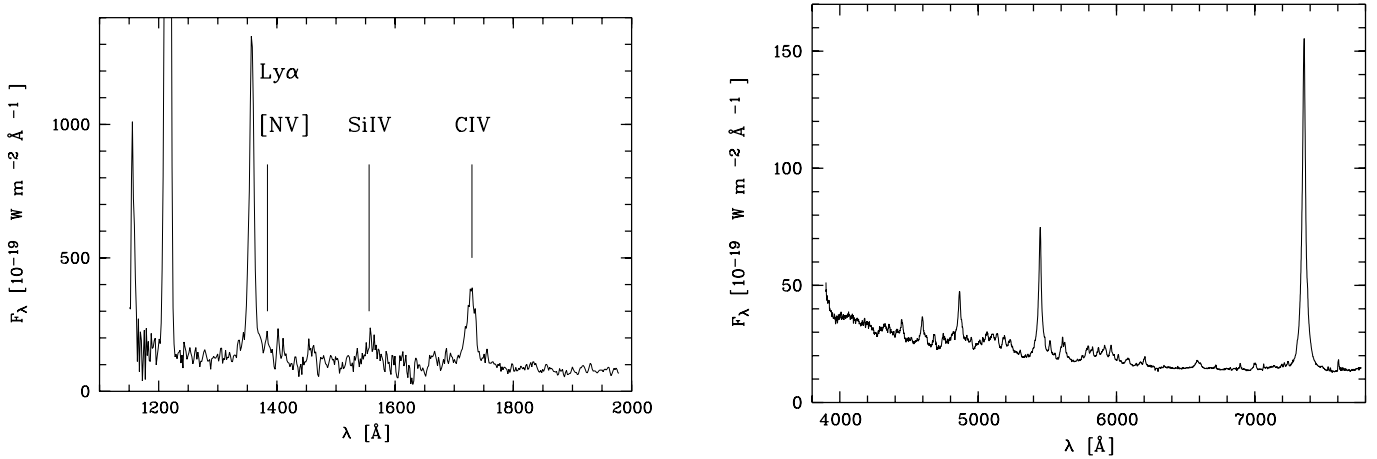[d] The upper limit of the NVSS observation is $\nu L_{1.4\,\mathrm{GHz}} < 4.7 \times 10^{31}$ W.

FIG. 11.—*IUE* and optical spectra of RX J0148.3−2758.

REFERENCES

Aoki, K., Kawaguchi, T., & Ohta, K. 2005, ApJ, 618, 601
Arnaud, K. A. 1996, in ASP Conf. Ser. 101, Astronomical Data Analysis Software, ed. G. H. Jacoby & J. Barnes (San Francisco: ASP), 17
Barthelmy, S. D. 2005, Space Sci. Rev., 120, 143
Belloni, T., Hasinger, G., & Izzo, C. 1994, A&A, 283, 1037
Beuermann, K., Thomas, H.-C., Reinsch, K., Schwope, A. D., Trümper, J., & Voges, W. 1999, A&A, 347, 47
Bian, W., Yuan, Q., & Zhao, Y. 2005, MNRAS, 364, 187
Boller, T., Brandt, W. N., & Fink, H. H. 1996, A&A, 305, 53
Boroson, T. A. 2002, ApJ, 565, 78
Boroson, T. A., & Green, R. F. 1992, ApJS, 80, 109
Brandt, W. N., Mathur, S., & Elvis, M. 1997, MNRAS, 285, L25
Burrows, D. N., et al. 2005, Space Sci. Rev., 120, 165
———. 2006, ApJ, submitted (astro-ph/0604320)
Chiang, J., Reynolds, C. S., Blaes, O. M., Nowak, M. A., Murray, N., Madejeski, G., Marshall, H. L., & Magdziarz, P. 2000, ApJ, 528, 292
Dewangan, G. C., Boller, Th., Singh, K. P., & Leighly, K. M. 2002, A&A, 390, 65
Dickey, J. M., & Lockman, F. J. 1990, ARA&A, 28, 215
Elvis, M., Risaliti, G., Nicastro, F., Miller, J., Fiore, F., & Puccetti, S. 2004, ApJ, 615, L25
Fabian, A. C., Miniutti, G., Gallo, L. C., Boller, Th., Tanaka, Y., Vaughan, S., & Ross, R. 2004, MNRAS, 353, 1071
Ferrarese, L., & Merritt, D. 2000, ApJ, 539, L9
Gallo, L. C. 2006, MNRAS, 368, 479
Gallo, L. C., Boller, Th., Brandt, W. N., Fabian, A. C., & Grupe, D. 2004a, MNRAS, 352, 744
Gallo, L. C., Tanaka, Y., Boller, Th., Fabian, A. C., Vaughan, S., & Brandt, W. N. 2004b, MNRAS, 353, 1064
Gebhardt, K., et al. 2000, ApJ, 539, L13
Gehrels, N., et al. 2004, ApJ, 611, 1005
Gliozzi, M., Brinkmann, W., O'Brien, P. T., Reeves, J. N., Pounds, K. A., Trioglio, M., & Gianotti, F. 2001, A&A, 365, L128
Goodrich, R. W. 1989, ApJ, 342, 224
Grupe, D. 1996, Ph.D. thesis, Univ. Göttingen
———. 2004, AJ, 127, 1799
Grupe, D., Beuermann, K., Mannheim, K., & Thomas, H.-C. 1999, A&A, 350, 805
Grupe, D., Beuermann, K., Thomas, H.-C., Mannheim, K., & Fink, H. H. 1998a, A&A, 330, 25
Grupe, D., & Leighly, K. M. 2002, in Workshop on X-Ray Spectroscopy of AGN with *Chandra* and *XMM-Newton*, ed. T. Boller (Garching: MPE), 287
Grupe, D., Leighly, K. M., Burwitz, V., Predehl, P., & Mathur, S. 2004a, AJ, 128, 1524
Grupe, D., Leighly, K. M., Thomas, H.-C., & Laurent-Muehleisen, S. A. 2000, A&A, 356, 11
Grupe, D., & Mathur, S. 2004, ApJ, 606, L41
Grupe, D., Mathur, S., & Komossa, S. 2004b, AJ, 127, 3161
Grupe, D., Thomas, H.-C., & Beuermann, K. 2001, A&A, 367, 470
Grupe, D., Wills, B. J., Leighly, K. M., & Meusinger, H. 2004c, AJ, 127, 156
Grupe, D., Wills, B. J., Wills, D., & Beuermann, K. 1998b, A&A, 333, 827
Hill, J. E., et al. 2004, Proc. SPIE, 5165, 217
Hogg, D. 1999, preprint (astro-ph/9905116)
Komossa, S., & Fink, H. H. 1997a, A&A, 327, 483
———. 1997b, A&A, 327, 555
Komossa, S., & Meerschweinchen, J. 2000, A&A, 354, 411
Laor, A., Fiore, F., Elvis, M., Wilkes, B. J., & McDowell, J. C. 1994, ApJ, 435, 611
———. 1997, ApJ, 477, 93

Lee, J. C., Fabian, A. C., Reynolds, C. S., Brandt, W. N., & Iwasawa, K. 2000, MNRAS, 318, 857
Leighly, K. M. 1999a, ApJS, 125, 297
———. 1999b, ApJS, 125, 317
Markwardt, C. B., Tueller, J., Skinner, G. K., Gehrels, N., Barthelmy, S. D., & Mushotzky, R. F. 2005, ApJ, 633, L77
Mason, K. O., et al. 2001, A&A, 365, L36
Mathur, S. 2000, MNRAS, 314, L17
Mathur, S., & Grupe, D. 2005a, A&A, 432, 463
———. 2005b, ApJ, 633, 688
Nandra, K., George, I. M., Mushotzky, R. F., Turner, T. J., & Yaqoob, T. 1997, ApJ, 476, 70
Nousek, J. A., et al. 2006, ApJ, 642, 389
Osterbrock, D. E., & Pogge, R. W. 1985, ApJ, 297, 166
Parsons, A., et al. 2005, GCN Circ. 4363, http://gcn.gsfc.nasa.gov/gcn3/4363.gcn3
Pfeffermann, E., et al. 1987, Proc. SPIE, 733, 519
Pounds, K. A., Done, C., & Osborne, J. P. 1995, MNRAS, 277, L5
Pounds, K. A., Reeves, J. N., Page, K. L., & O'Brien, P. T. 2004, ApJ, 616, 696
Puccetti, S., Risaliti, G., Fiore, F., Elvis, M., Nicastro, F., Perola, G. C., & Capalbi, M. 2004, Nucl. Phys. B Suppl., 132, 225
Puchnarewicz, E. M., Mason, K. O., Siemiginowska, A., & Pounds, K. A. 1995, MNRAS, 276, 20
Puchnarewicz, E. M., et al. 1992, MNRAS, 256, 589
Risaliti, G., Elvis, M., Fabbiano, G., Baldi, A., & Zezas, A. 2005, ApJ, 623, L93
Risaliti, G., Elvis, M., & Nicastro, F. 2002, ApJ, 571, 234
Rodríguez-Pascual, P. M., Mas-Hesse, J. M., & Santos-Lleó, M. 1997, A&A, 327, 72
Roming, P. W. A., et al. 2005, Space Sci. Rev., 120, 95
Schwope, A. D., et al. 2000, Astron. Nachr., 321, 1
Shields, G. A. 1978, Nature, 272, 706
Strateva, I. V., Brandt, W. N., Schneider, D. P., Vanden Berk, D. G., & Vignali, C. 2005, AJ, 130, 387
Sulentic, J. W., Zwitter, T., Marziani, P., & Dultzin-Hacyan, D. 2000, ApJ, 536, L5
Tanaka, Y., Boller, Th., Gallo, L. C., Keil, R., & Ueda, Y. 2004, PASJ, 56, L9
Tananbaum, H., et al. 1979, ApJ, 234, L9
Thomas, H.-C., Beuermann, K., Reinsch, K., Schwope, A. D., Trümper, J., & Voges, W. 1998, A&A, 335, 467
Tremaine, S., et al. 2002, ApJ, 574, 740
Trümper, J. 1982, Adv. Space Res., 2, 241
Turner, M. J. L., et al. 2001, A&A, 365, L27
Turner, T. J., George, I. M., Nandra, K., & Turcan, D. 1999, ApJ, 524, 667
Vaughan, S., Edelson, R., Warwick, R. S., Malkan, M. A., & Goad, M. R. 2001, MNRAS, 327, 673
Vaughan, S., Reeves, J., Warwick, R., & Edelson, R. 1999, MNRAS, 309, 113
Vestergaard, M., & Peterson, B. M. 2006, ApJ, 641, 689
Voges, W., et al. 1999, A&A, 349, 389
Walter, R., & Fink, H. H. 1993, A&A, 274, 105
Williams, R. J., Pogge, R. W., & Mathur, S. 2002, AJ, 124, 3042
Yuan, M. J., & Wills, B. J. 2003, ApJ, 593, L11
Yuan, W., Brinkmann, W., Siebert, J., & Voges, W. 1998a, A&A, 330, 108
Yuan, W., Siebert, J., & Brinkmann, W. 1998b, A&A, 334, 498
Zamanov, R., Marziani, P., Sulentic, J. W., Galvani, M., Dultzin-Hacyan, D., & Bachev, R. 2002, ApJ, 576, L9
Zimmermann, U., Boese, G., Becker, W., Belloni, T., Döbereiner, S., Izzo, C., Kahabka, P., & Schwentker, O. 1998, EXSAS User's Guide (Garching: *ROSAT* Scientific Data Center), http://wave.xray.mpe.mpg.de/exsas/users-guide